Environmental Pollution 243 (2018) 37–48

Contents lists available at ScienceDirect

Environmental Pollution

journal homepage: www.elsevier.com/locate/envpol

Baseline characterisation of source contributions to daily-integrated $PM_{2.5}$ observations at Cape Grim using Radon-222☆

Jagoda Crawford*, Scott D. Chambers, David D. Cohen, Alastair G. Williams, Armand Atanacio

Australian Nuclear Science and Technology Organisation, Locked Bag 2001, Kirrawee DC, NSW, 2232, Australia

ARTICLE INFO

Article history:
Received 8 March 2018
Received in revised form
18 June 2018
Accepted 16 August 2018
Available online 20 August 2018

Keywords:
Aerosols
Radon
Cape Grim
Baseline

ABSTRACT

We discuss 15 years (2000–2015) of daily-integrated $PM_{2.5}$ samples from the Cape Grim Station. Ion beam analysis and positive matrix factorisation are used to identify six source-type fingerprints: fresh sea salt (57%); secondary sulfate (14%); smoke (13%); aged sea salt (12%); soil dust (2.4%); and industrial metals (1.5%). An existing hourly radon-only baseline selection technique is modified for use with the daily-integrated observations. Results were not significantly different for days on which >20 hours were below the baseline radon threshold compared with days when all 24 hours satisfied the baseline criteria. This relaxed daily baseline criteria increased the number of samples for analysis by almost a factor of two. Two radon baseline thresholds were tested: historic (100 mBq m^{-3}), and revised (50 mBq m^{-3}). Median aerosol concentrations were similar for both radon thresholds, but maximum values were higher for the 100 mBq m^{-3} threshold. Back trajectories indicated more interaction with southern Australia and the Antarctic coastline for air masses selected with the 100 mBq m^{-3} threshold. Radon-only baseline selection using the 50 mBq m^{-3} threshold was more selective of minimal terrestrial influence than a similar recent study using wind direction and back trajectories. The ratio of concentrations between terrestrial and baseline days for the primary sources soil, smoke and industrial metals was 3.4, 2.6, and 5.5, respectively. Seasonal cycles of soil dust had a summer maximum and winter minimum. Seasonal cycles of smoke were of similar amplitude for terrestrial and baseline events, but of completely different shape: peaking in autumn and spring for terrestrial events, compared to summer for baseline conditions. Seasonal cycles of industrial metals had a summer maximum and winter minimum. A significant fraction of the Cape Grim baseline smoke and industrial metal contributions appeared to be derived from long-term transport (>3 weeks since last terrestrial influence).

1. Introduction

Particulate matter (PM) in the atmosphere can affect climate either directly, through the scattering and absorption of short and long wave radiation, or indirectly, by modifying cloud properties (Rotstayn et al., 2009). Knowledge of trends in the PM concentration of earth's atmosphere is therefore important in climate change studies.

Atmospheric PM can arise from either natural sources (e.g. sea salt, soil dust, emissions from volcanoes) or anthropogenic sources (e.g. coal-burning, metal smelting and vehicle emissions) (Fleming et al., 2012; Liang et al., 2016). To help determine trends in PM concentrations some measurement sites are situated close to sources of particular interest (e.g., adjacent to roads or point sources in urban areas; over oceans, in forests or peat bogs for marine, rural or biogenic emissions; Flemming et al., 2012). However, long term changes in PM concentrations of aged, well-mixed air masses, and long-range PM transport, are also of considerable interest, for which background or “baseline” sites are required.

Atmospheric PM measurement programs have been established at global “baseline” stations (WMO/GAW, 2017) with the aim of characterising the long-term trends of regional background atmospheric PM pollution (WMO, 1978). Given the contrasting physical settings of the various WMO GAW baseline stations, an important component of these measurement programs are tools and techniques that enable a distinction to be made between air masses

☆ This paper has been recommended for acceptance by Haidong Kan.

* Corresponding author.
E-mail address: Jagoda.Crawford@ansto.gov.au (J. Crawford).

https://doi.org/10.1016/j.envpol.2018.08.043
0269-7491/

representative of the well-mixed background atmosphere, and those that have been influenced "recently" (e.g. within the past 2–3 weeks) by localised sources.

Traditionally, "baseline" (aged, well-mixed air) selection techniques have relied upon combinations of meteorological conditions and statistical tools (e.g. Thoning et al., 1989; Galbally and Schultz, 2013; Hyslop et al., 2013; Chambers et al., 2013). At the Cape Grim Baseline Air Pollution Station (CGBAPS), for example, baseline air masses have mainly been selected according to wind direction (the sector between 190° and 280°) and wind speed (≥20 km/h; Ayers and Ivey, 1988; Molloy and Galbally, 2014). Galbally and Schultz (2013) provided a more comprehensive list of criteria that could be used to identify representative air masses for tropospheric ozone measurements, which include: wind speed and direction; particle number concentration; radon concentration; air mass back trajectories; mole fractions of other trace species, notably CO; tracer/tracer mole fraction ratios; criteria based on statistical time series analyses.

Fleming et al. (2012) undertook a review of methods used to determine the origin and pathway of air masses sampled at a pollution monitoring location (e.g., wind roses, synoptic weather systems, back trajectories and dispersion modelling). They point out that the main disadvantage with the use of wind roses is that one cannot assume that the wind direction measured at a point is consistent with the synoptic scale flow. Using back trajectories to calculate the average atmospheric motion of an air mass offers an improvement over wind roses, however their accuracy is affected by the resolution of the meteorological data used for their calculations, and these errors increase with the hind-cast distance. Particle dispersion models, which trace multiple particles, are more accurate; however in both cases a decision needs to be made on the length of time for which to trace the back trajectory.

An alternative to traditional baseline selection techniques that is gaining acceptance is the use of the terrestrial tracer species Radon-222 (radon); either alone (Griffiths et al., 2016; Chambers et al., 2016; Giemsa et al., 2017), or in conjunction with back trajectory analysis (e.g. Zahorowski et al., 2013; Chambers et al., 2014; Molloy and Galbally, 2014). Radon is a naturally occurring radioactive gas originating exclusively from the earth's surface. Being a noble gas, with a well-distributed, relatively consistent source function, it has been widely used as a sensitive, unambiguous indicator of recent terrestrial influences on air masses (e.g. Liu et al., 1984; Polian et al., 1986; Chambers et al., 2014, 2016; and references therein). The radon terrestrial source function (for unsaturated/unfrozen conditions) is 2–3 orders of magnitude greater than that from extensive water bodies (e.g. Wilkening and Clements, 1975; Schery et al., 1989). With a half-life of 3.8 days, it can be used to indicate the recent (2–3 week) history of an air mass, but does not accumulate in the atmosphere for longer timescales.

Chambers et al. (2016) demonstrated that at CGBAPS, where the lower limit of detection for radon is currently <10 mBq m^{-3} (Williams and Chambers, 2016), an appropriate radon concentration threshold for the identification of baseline air masses is 40 mBq m^{-3}. It should be noted, however, that a correction to the CGBAPS primary radon detector's flow meter since this publication has resulted in a revision of this threshold value to ~50 mBq m^{-3}. Using this detection threshold, and an appropriately sensitive detector, radon alone can be effectively used as a baseline selection tool. The operational characteristics of prior models of radon detector operating at CGBAPS necessitated a radon threshold of 100 mBq m^{-3} to be adopted; a threshold that needed to be applied in conjunction with traditional baseline selection tools (e.g. Molloy and Galbally, 2014).

Crawford et al. (2017) characterised 24-h integrated $PM_{2.5}$ concentrations associated with baseline air masses at CGBAPS selected using a combination of wind direction and back-trajectory analysis. In this study we modify the radon-only baseline selection approach, based on hourly observations (Chambers et al., 2016), for application to daily-integrated $PM_{2.5}$ measurements, and compare our findings with the back-trajectory method of Crawford el al. (2017). A similar approach can be used to develop a technique applicable at other baseline stations as well as coastal sites.

2. Study site and methods

2.1. Study site

Cape Grim Baseline Air Pollution Station is located at the north western tip of Tasmania (40°41′S, 144°41′W), an island about 200 km south of the Australian mainland. The station is located on top of a 94 m high cliff, overlooking the Southern Ocean to the south-west. Meteorological, trace gas, and atmospheric radon concentrations are monitored from an adjacent 70 m telecommunications tower (Cleland, 2014), whereas all PM observations are made from a platform on the roof of the station 94 m above ground level (Station Specification, 2014).

2.2. Aerosol sampling and elemental analysis

ANSTO has collected discrete filter samples of $PM_{2.5}$ at Cape Grim since 1998 using an IMPROVE $PM_{2.5}$ cyclone system (Cohen et al., 1996). This system employs a 25 mm diameter Teflon filter and typically samples at a flow rate of 22 L/min. Twenty-four-hour (midnight-to-midnight) continuous $PM_{2.5}$ samples are collected twice a week (Wednesday and Sunday). After sample collection, accelerator-based ion beam analysis (IBA) is used to determine the elemental composition of the $PM_{2.5}$ samples (Cohen et al., 1996). The concentrations of 22 elements are determined for each sample (H, N, Na, Al, Si, P, S, Cl, K, Ca, Ti, V, Cr, Mn, Fe, Co, Ni, Cu, Zn, Se, Br and Pb). Additionally, a laser HeNe absorption system, assuming a mass adsorption coefficient of 7 m^2/g is used to determine the black carbon (BC) concentrations.

Source type fingerprints were determined using PMF (Paatero and Tapper, 1994), which solves the standard bi-linear factor analysis model. The PMF method can result in a number of possible solutions which the user has to choose from based on errors of the fit (Q value) and how well the factors represent known source types. In this application, between four and seven source fingerprints were examined and it was found that the solution with six source fingerprints best explained the known source types. The expected Q value is the degrees of freedom of the problem; i.e. nm-p(n + m) (Paatero and Tapper, 1994). Here n (the number of data points) was 1708, m (the number of elements) was 23 and selected solution had a p (number of source types to be resolve) of 6. This implies an expected Q of 28,898; however the final Q was 13411 (about 46% of the expected Q), which would indicate that perhaps too many fingerprints were resolved. However, this was not supported as there was no correlation between the resolved fingerprints. Hence, six fingerprints were used for the analysis, details of which are provided in Crawford et al. (2017). To summarise, fresh sea salt (*Sea*) contributed to 57% of the measured $PM_{2.5}$ mass; secondary sulfate and nitrates (*2ndryS*), smoke from biomass burning (*Smoke*), aged sea air (*SeaAged*; the product of NaCl reactions with SO_2), soil dust (*Soil*), and industrial metals (*Indmetals*), contributed to14, 13, 12, 2.4 and 1.5% to the measured $PM_{2.5}$ mass, respectively.

2.3. Radon measurements and daily baseline definition

Direct, hourly atmospheric radon concentrations at Cape Grim

are measured using the dual-flow-loop, two-filter method (e.g. Whittlestone and Zahorowski, 1998; Chambers et al., 2014; Griffiths et al., 2016). There have been many changes to the atmospheric radon detection system at Cape Grim since measurements began in 1980, all of which have been summarised in Williams and Chambers (2016). The performance and operational characteristics of the present detection system have been discussed in Zahorowski et al. (2013) and Williams and Chambers (2016).

In February 2017 an adjustment was made to the calibration of the primary Cape Grim radon detector's flow meter, resulting in a revision of the 20–40 mBq m^{-3} radon concentration range for air masses thought to have been in long-term equilibrium with the Southern Ocean (see Chambers et al., 2016), up to 30–50 mBq m^{-3}. Air masses with radon concentrations <30 mBq m^{-3} are thought to be admixtures of marine boundary layer (MBL) with tropospheric (or stratospheric) air (Chambers et al., 2018), or air recently transported from Antarctic regions (e.g. Zahorowski et al., 2013). As demonstrated by Chambers et al. (2015), this revised 50 mBq m^{-3} radon baseline threshold for CGBAPS observations constitutes a significant improvement over the previously employed threshold of 100 mBq m^{-3} to help characterise baseline concentrations of atmospheric trace species (e.g. Molloy and Galbally, 2014). A recent analysis of 4 years of hourly radon and carbon dioxide observations at CGBAPS and Macquarie Island by Williams et al. (2017) also highlighted the potential influence of vestigial terrestrial influences (radon concentrations as low as 80–100 mBq m^{-3}) on would-be baseline observations.

Whilst CGBAPS baseline studies have generally utilised observations with hourly temporal resolution, the intention here is to analyse 24-h integrated $PM_{2.5}$ samples from the ANSTO IMPROVE system. While the twice-weekly $PM_{2.5}$ data is available from 1998 to 2016, a 15-year subset of this data (2000–2015) has been chosen for this investigation, as this corresponds to the period of availability of excellent quality data from the modern generation of high sensitivity 5000L radon detectors at Cape Grim ("HURD2&3") with high efficiency measurement heads and LLD < 10 mBq m^{-3} (Williams and Chambers, 2016). Over this period there were a total of 1493 valid daily $PM_{2.5}$ samples collected and analysed.

Given the $PM_{2.5}$ data was available on a daily basis we sought to determine the minimum number of hourly samples each day that had to satisfy our "baseline" criteria (based on the radon thresholds) in order for the entire day's $PM_{2.5}$ sample to be considered representative of baseline conditions. This analysis was required in order to maximise the number of $PM_{2.5}$ samples that could be analysed under baseline conditions and thus improve the associated statistical analysis. This was achieved by considering the eight distinct categories below:

Category #0: 0 of 24 h in baseline (full continental influence)
Category #1: <4 of 24 h in baseline
Category #2: 4–8 of 24 h in baseline
Category #3: 8–12 of 24 h in baseline
Category #4: 12–16 of 24 h in baseline
Category #5: 16–20 of 24 h in baseline
Category #6: >20 of 24 h in baseline
Category #7: 24 of 24 h in baseline (full baseline)

where "baseline" is simply defined as a radon concentration below a given threshold. A 4 h grouping was used to ensure sufficient data was available within each group to carry out statistical analyses. To highlight the difference between the historical (100 mBq m^{-3}) and recent (50 mBq m^{-3}) radon concentration thresholds used for baseline identification, we will duplicate our analyses to present results based on both thresholds.

2.4. Back trajectory analysis

Back-trajectories for the current study were generated using HYSPLIT v4.0 (HYbrid Single-Particle Lagrangian Integrated Trajectory; Draxler et al., 2016; Stein et al., 2015), and a starting height of 300 m above ground level (intended to be well within the typical extent of the MBL inversion in this region, ~400–600 m; Zahorowski et al., 2013). Source data for the trajectory modelling was the 1^{o}x1^{o} meteorological dataset generated by the global data assimilation system (GDAS) model run by the National Weather Service's (NWS) National Centre for Environmental Prediction (NCEP; available at ftp://arlftp.arlhq.noaa.gov/archives/gdas1). Due to the period for which the meteorological data was available, back trajectory plots were generated only from January 2001 onwards.

Regarding the presentation of back-trajectories in this study, 10-day back-trajectories were generated for each of the 24 h of each day of $PM_{2.5}$ sampling. Back-trajectory density maps were then generated, for which the horizontal position of the back-trajectory (or trajectory endpoint) was determined every 30 min. The region was sub-dividend into grid cells of 0.5° by 0.5° dimension, and if a back-trajectory endpoint landed in the grid cell, a grid cell counter was incremented.

3. Results and discussion

3.1. Initial baseline selection

A total of 1493 $PM_{2.5}$ samples were available. Strictly imposing the rule that all 24 hourly radon concentrations for each aerosol sampling day had to be below the 100 mBq m^{-3} baseline radon threshold reduced the number of $PM_{2.5}$ samples remaining for analysis to 285. Then in the second case where the baseline radon threshold of 50 mBq m^{-3} was used, the number of samples was reduced to 90. To determine whether it was possible to improve the robustness of our baseline statistics, without seriously compromising the quality of our baseline characterisation, we performed a sensitivity analysis of the total $PM_{2.5}$ (and each source fingerprint) for each of the eight categories of sampling event outlined in Section 2.3.

A paired *t*-test was performed to test the significance of the difference in mean values between all 8 data categories (for each source fingerprint). Differences were significant for all combinations of categories except between category 6 and category 7 events. Due to these sensitivity tests, only the statistics for category 0, 6 and 7 events are summarised in Tables 1a and 1b alongside the corresponding statistics for all data.

Relaxing our baseline requirement from 24 h in baseline (category 7) to >20 h in baseline (category 6) for each aerosol sampling day increased the number of available samples for the 100 mBq m^{-3} radon threshold from 285 to 382 without a statistically significant change in the resulting baseline concentrations. When the baseline radon threshold of 50 mBq m^{-3} was used, the number of samples was increased from 90 to 173. Based on this result it is evident that in cases where insufficient data is available from category 7 events (24 h in baseline), then measurements of category 6 events (>20 h in baseline) should enable suitable characterisation of baseline $PM_{2.5}$ concentrations.

Consequently, final baseline statistics for aerosol samples will be prepared based on category 6 daily events.

Assuming radon concentration to be a suitable proxy for terrestrial influence on an air mass, a relative indication of the degree of terrestrial influence on the 24-h integrated $PM_{2.5}$ samples collected within our measurement categories 1–6 (i.e. not including full terrestrial or full baseline categories) was determined by calculating distributions of radon concentration of the

Table 1
Statistics for different sources (aerosols in μg/m^3 and radon in mBq/m^3; the number of samples is given in brackets).

Table 1a: when an Rn threshold of 100 mBq/m3 was used for baseline conditions

Source	All data (1493)			24 h terrestrial (459)			>20 h in baseline (382)			24 h in baseline (285)		
	Mean	Min	Max	Mean	Min	Max	Mean	Min	Max	Mean	Min	Max
Rn	579.2	0	5922.8	1293.1	138	5922.8	42.2	0	178.3	37.1	0	73.1
$PM_{2.5}$ (all)	5.58	0.62	16.95	5.4	0.62	16.08	5.45	0.78	14.12	5.42	0.78	14.12
Sea	3.28	0	12.98	1.95	0	9.25	4.19	0.64	12.48	4.16	0.64	10.67
2ndryS	0.8	0	7.47	1.19	0	7.47	0.56	0	3.77	0.54	0	2.78
SeaAged	0.6	0	4.93	0.88	0	4.93	0.33	0	1.45	0.32	0	1.45
Smoke	0.7	0	5.98	1.05	0	5.98	0.38	0	4.26	0.38	0	4.26
Soil	0.13	0	2.04	0.17	0	0.8	0.05	0	0.29	0.05	0	0.29
Indmetals	0.07	0	1.16	0.14	0	1.16	0.02	0	0.57	0.02	0	0.57

Table 1b: when an Rn threshold of 50 mBq/m3 was used for baseline conditions

Source	All data (1493)			24 h terrestrial (732)			>20 h in baseline (173)			24 h in baseline (90)		
	Mean	Min	Max	Mean	Min	Max	Mean	Min	Max	Mean	Min	Max
Rn	579.2	0	5922.8	971.6	64.63	5922.8	27.9	0	178.3	22.3	0	41.4
$PM_{2.5}$ (all)	5.58	0.62	16.95	5.57	0.62	16.95	5.07	0.78	13.42	4.86	0.78	11.44
Sea	3.28	0	12.98	2.54	0	11.58	3.91	0.64	12.48	3.8	0.7	9.13
2ndryS	0.8	0	7.47	1.01	0	7.47	0.54	0	2.28	0.5	0	2.28
SeaAged	0.6	0	4.93	0.78	0	4.93	0.35	0	1.32	0.33	0	1.32
Smoke	0.7	0	5.98	0.92	0	5.98	0.35	0	0.93	0.36	0	0.93
Soil	0.13	0	2.04	0.17	0	2.04	0.05	0	0.29	0.05	0	0.29
Indmetals	0.07	0	1.16	0.11	0	1.16	0.02	0	0.57	0.03	0	0.57

remaining hours each day that were *not* in baseline (see Fig. 1). For example, for Category #1, if the hourly radon measurements were less than the baseline threshold for 3 h or less out of 24, the radon distribution for the reaming hours (i.e. for those hours when the measured radon was greater than the threshold) are presented in the first entry of Fig. 1a and b. This entry contains the highest radon measurements, as air masses would have received a terrestrial influence for a large fraction of the day.

By this method, the degree of terrestrial influence on our daily $PM_{2.5}$ samples was observed to reduce markedly from category 1 to category 6 events (i.e. with increasing time in baseline). The reduction in daily terrestrial influence was greater and more rapid in the case of the 50 mBq m^{-3} radon threshold (Fig. 1b). The fact that the radon concentration of non-baseline air masses each day reduced as the number of baseline air masses on that day increased is an indication that the transition from full baseline to full continental events is often gradual.

Despite the large, monotonic decline in terrestrial influence evident for category 1–6 events, no comparable trend was evident in the total $PM_{2.5}$ concentration distributions calculated for corresponding events (Fig. 2). This is evidence of the substantial contribution to the total $PM_{2.5}$ loading at CGBAPS from non-terrestrial sources, and highlights the necessity of a more detailed analysis of individual source fingerprints at this site. Figs. 3 and 4 replicate the analyses of Fig. 2(a and b) for each of the 6 identified source fingerprints (soil, smoke, industrial metals, fresh sea salt, aged sea salt, and secondary sulphur).

In the case of category 6 events (>20 h in baseline) the average radon concentration of non-baseline hours each day was >200 mBq m^{-3} on only 10 (of 382) occasions (~3%) when using the 100 mBq m^{-3} threshold, compared to ~1% (2 of 173) when using the 50 mBq m^{-3} threshold. This minimal level of terrestrial influence on these days is clearly reflected in the low concentrations and compact distributions of the $PM_{2.5}$ contributions from primary sources of

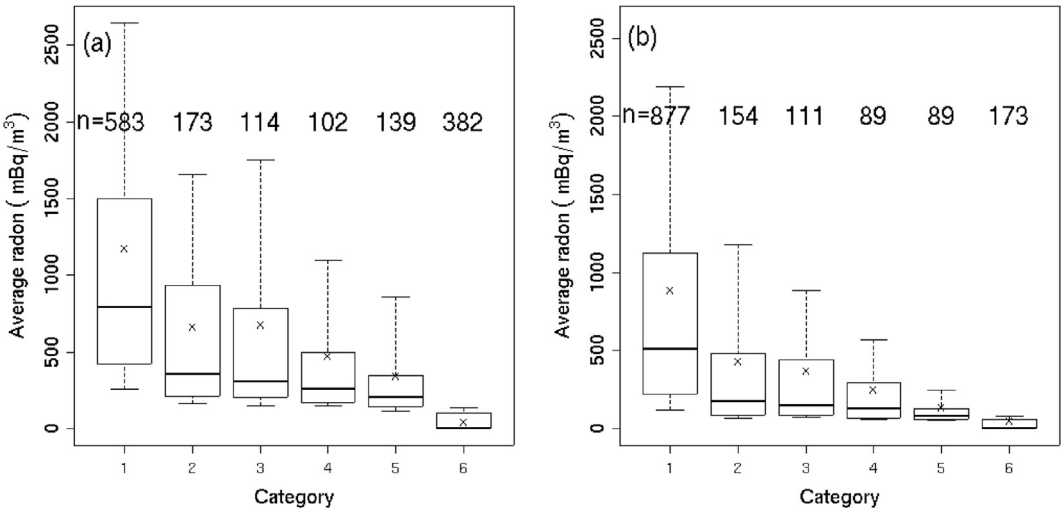

Fig. 1. Radon concentration distributions for non-baseline hours of category 1–6 events for radon baseline thresholds of (a) 100 mBq m^{-3}, and (b) 50 mBq m^{-3} (line is median, boxes 1st and 3rd quartiles, dashed lines 10th and 90th percentiles, "X" represents the mean, and n is the number of samples).

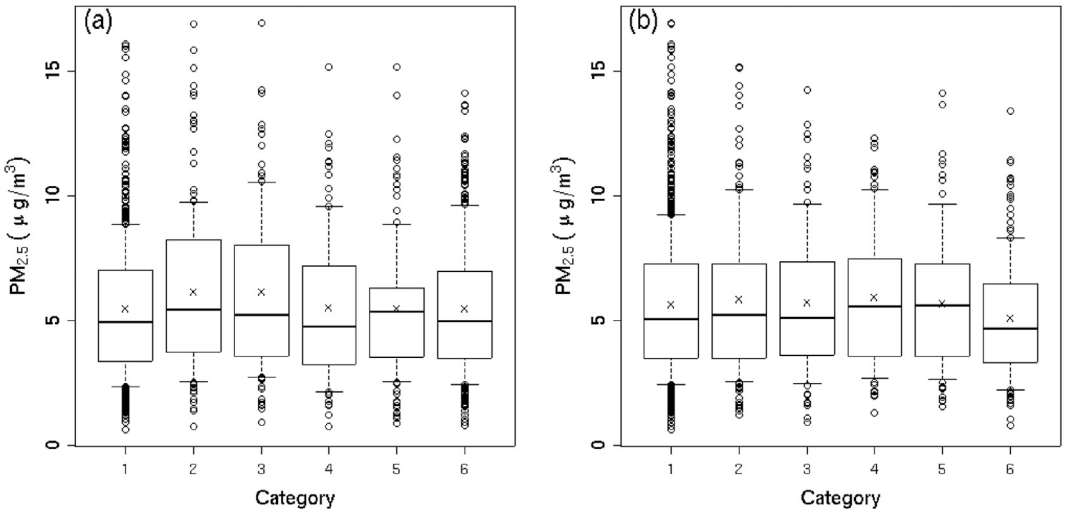

Fig. 2. Distributions of total $PM_{2.5}$ concentration in category 1–6 events for radon threshold values of (a) 100 mBq m^{-3}, and (b) 50 mBq m^{-3} (symbols as for Fig. 1 with outliers represented by open circles).

predominantly terrestrial origin (i.e. soil, smoke, and industrial metals) shown in Fig. 3. As was the case for radon, concentrations of these $PM_{2.5}$ contributing species demonstrate a large and relatively consistent decrease with decreasing terrestrial influence.

Similar to the behaviour of the terrestrial sources, concentrations of the aged sea salt marker (*SeaAged*; Fig. 4) also decreased substantially (approximately factor of two from category 1 to 6 events) and relatively consistently with reducing terrestrial influence. By contrast, concentrations of secondary sulphates (*2ndryS*; Fig. 4) were fairly similar for all but the most strongly terrestrially influenced events. It is known that gaseous dimethylsulfate (CH_3SCH_3; DMS) enters the marine atmosphere from the ocean (Ayers et al., 1997), where it undergoes a number of photochemical reactions. One of the intermediates is SO_2 which is then converted to sulfate aerosols. It has been estimated that anthropogenic and the emission of DMS from the oceans accounts for 70% and 25%, respectively, of the SO2 precursors leading to the formation of secondary sulpfate (Faloona, 2009). However the DMS estimates have a large uncertainty.

As expected, the contribution to total $PM_{2.5}$ by fresh sea salt (Fig. 4) progressively increases from category 1 to category 6 events (reducing terrestrial influence) for the radon threshold of 100 mBq m^{-3}. Interestingly, however, in the case of the 50 mBq m^{-3} threshold there is a slight reduction in the median fresh sea salt contribution going from category 5 to category 6 events. This is possibly due to an increased proportion of tropospheric MBL intrusion events that are typically characterised by radon concentrations between 0 and 30 mBq m^{-3} (Chambers et al., 2015).

The difference in the means between the different categories was more significant for those samples when air masses were arriving from the baseline for 16–20 h of the sampling day (Category 5) to those when all 24 h were identified as baseline air masses, with the difference in the means of *Smoke* being significant at 95% level and the others at a slightly lower confidence level.

A further paired *t*-test was applied to means when either 100 or 50 mBq m^{-3} was used for baseline conditions. This test indicated that category means for all $PM_{2.5}$ source components were not significantly different based on whether a radon threshold of 100 or 50 mBq m^{-3} was used. A corollary of this result is that in the case of mean values of 24-h integrated $PM_{2.5}$ observations radon-derived baseline selection can be made equally effectively using either a 100 or 50 mBq m^{-3} baseline threshold. However, for some $PM_{2.5}$ source contributions (e.g. secondary sulphur and smoke), maximum observed values were much higher when the 100 mBq m^{-3} radon threshold value was used than with the 50 mBq m^{-3} value.

Based on the more stringent 50 mBq m^{-3} radon baseline threshold, the ratio of mean source concentrations between category 0 (fully continental) and category 6 events (Table 1b) was: 3.4, 2.6, 5.5, 2.2, 1.9, and 0.7, for *Soil, Smoke*, *Indmetals*, *SeaAged*, *SndryS*, and *Sea*, respectively. The largest contrasts were seen for industrial metals, soil and smoke.

The values in Table 1b compare well to those reported in Table 2 of Crawford et al. (2017) which were generated by using only wind direction and back trajectories as baseline indicators. However, the radon method produced lower median values for soil and aged sea air (see Section 3.4 for details).

3.2. Fetch analysis of baseline events

Back-trajectory density maps showing the fetch history of hourly Cape Grim air masses beneath the concentration thresholds of 100 and 50 mBq m^{-3} are presented in Fig. 5a and b and categories 0 to 5 in Fig. 5c. In the case of air masses below the 100 mBq m^{-3} threshold (Fig. 5a), frequent interaction with NW Tasmania is evident, as well as occasional interaction with the southern fringes of mainland Australia. By contrast, density maps prepared according to the 50 mBq m^{-3} radon threshold showed only occasional interaction of air masses with NW Tasmania, greatly reduced interaction with southern parts of Australia, and less frequent interaction with coastal Antarctic regions (where there can be exposed rock emitting radon). The combined categories 0 to 5 show more fetch from the Australian mainland.

3.3. Seasonal distribution of $PM_{2.5}$ sources

The distributions of concentrations, by season, for the more terrestrially affected and least terrestrially affected air masses are presented in Figs. 6 and 7, respectively.

The seasonal cycle of the $PM_{2.5}$ soil source contribution based on days with significant terrestrial influence (Fig. 6a) had an amplitude of 0.07 μg m^{-3} (based on median values), characterised by a summer maximum and winter minimum, corresponding to a higher degree of local Tasmanian fetch in summer (identified by back

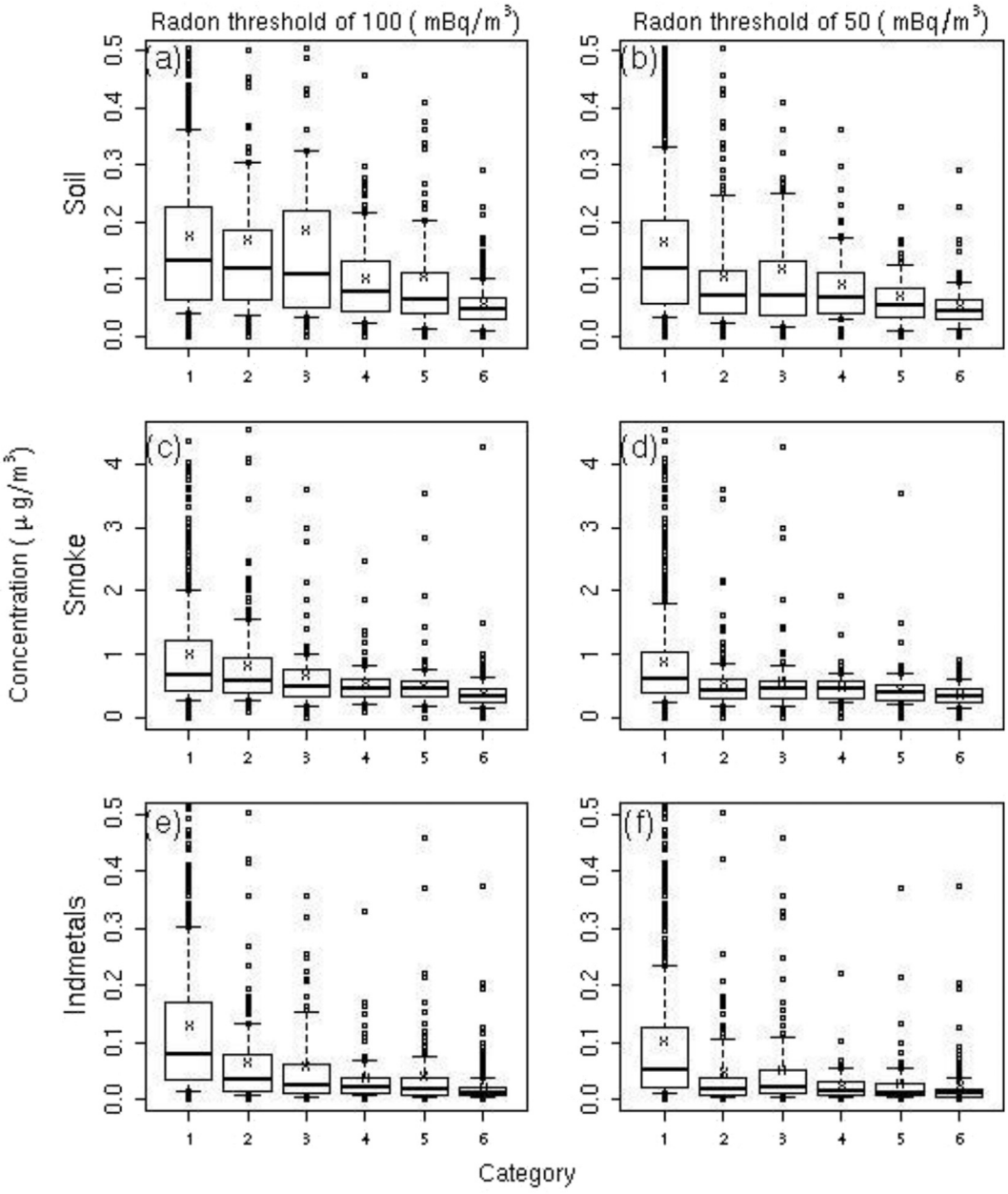

Fig. 3. Distributions of source fingerprint concentrations of category 1–6 events for baseline radon concentration threshold values of 100 mBq m^{-3} and 50 mBq m^{-3} (symbols as for Fig. 2).

trajectory studies in Crawford et al., 2017). By contrast, seasonal cycles of median concentrations for smoke and industrial metals showed peak values in autumn, secondary peak values in spring, with lower values in both summer and winter. The timing of these peaks seems to be more closely associated with anthropogenic biomass burning cycles (either of agricultural origin or related to prescribed burning for hazard reduction; Sustainable Timber Tasmania, 2017; and also from mainland sources, e.g. Victoria), rather than natural bushfires (which would produce a maximum in summer).

The seasonal cycle of the soil component of $PM_{2.5}$ within the baseline category (Fig. 7a), had an amplitude of 0.02 µg m^{-3} (based on median values), roughly 30% of the amplitude for terrestrial events, but also characterised by a summer maximum and winter minimum. This cycle appears to be similarly tied to the southern hemisphere growing season/soil moisture cycle but, based on Fig. 5b, is likely attributable to long-range transport. Li et al. (2008) indicate that the dust in the southern hemisphere originates mainly from Australia and Patagonia and some inter-hemispheric transport. Weller et al. (2013) also reported higher dust concentrations at the German Antarctic Station Neumayer in summer.

Regarding the smoke component of $PM_{2.5}$ within the baseline category (Fig. 7b), the seasonal cycle has a similar amplitude, but completely different shape to that observed for the significantly terrestrially influenced days. The baseline smoke seasonal cycle was characterised by a summer maximum and winter minimum. Unlike the days with significant terrestrial influence, the baseline smoke concentration appears to be more closely tied to the southern hemisphere bushfire cycle (e.g. Mari et al., 2008).

Under baseline conditions the seasonal cycle of median

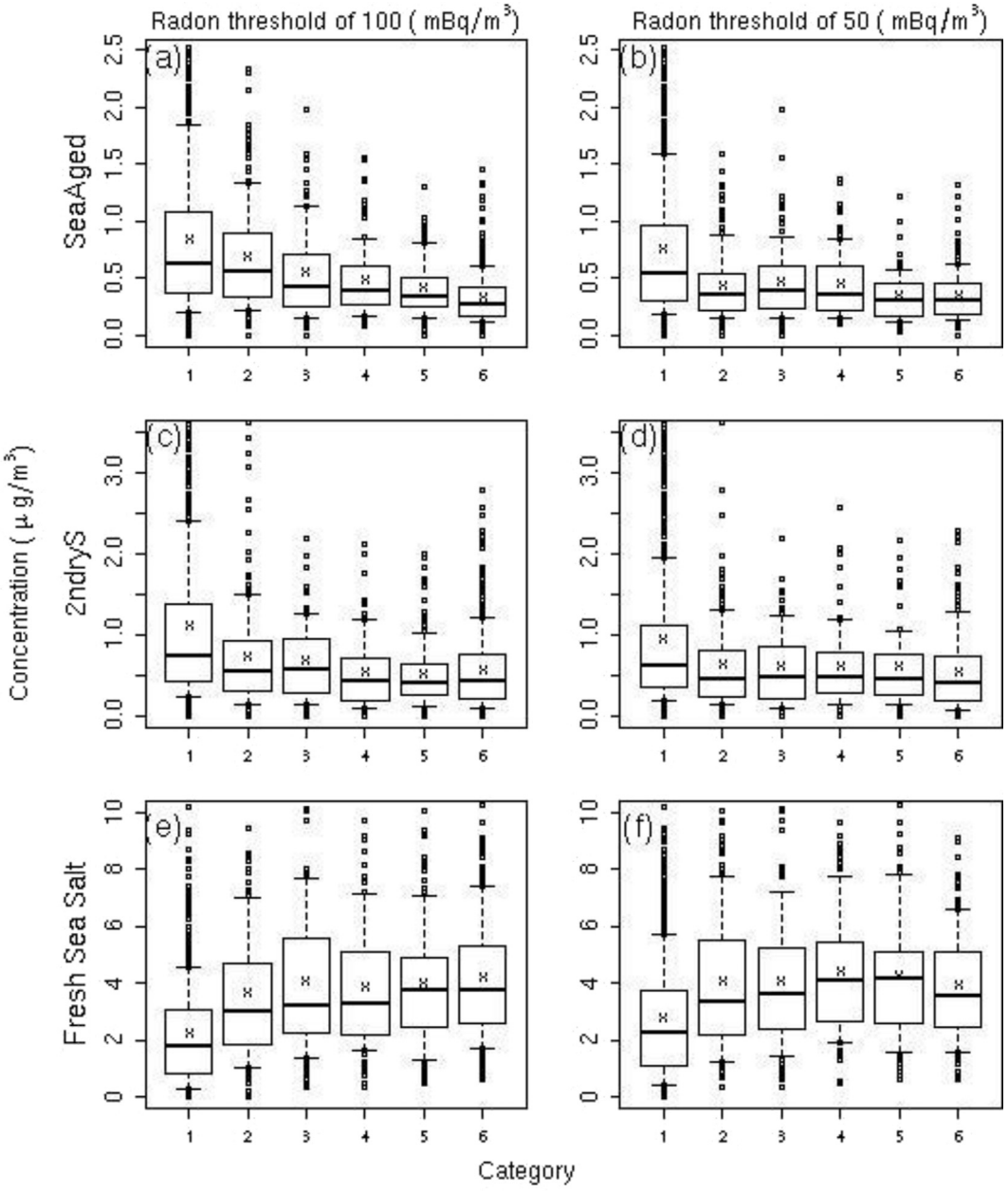

Fig. 4. Distributions of source fingerprint concentrations of category 1–6 events for baseline radon concentration threshold values of 100 mBq m^{-3} and 50 mBq m^{-3} (symbols as for Fig. 1).

concentrations of smoke, was characterised by a summer and spring maximum and winter minimum (Fig. 7c; a difference of 0.1 μg m^{-3}, or 28% of the summer median value). For significant terrestrial fetch the largest median value was recorded in autumn and the smallest in summer (Fig. 6c, a difference of 0.12 μg m^{-3}, or 20% of the autumn median value).

For predominantly terrestrial air masses the seasonal cycle of aged sea air had an amplitude of 0.4, and was characterised by a summer maximum and winter minimum. The seasonal cycle was similar under baseline conditions, but lower variability within seasons. Ayers et al. (1999) undertook a study of Chloride (Cl^-) and Bromide (Br^-) loss from sea-salt particles in the Southern Ocean air, and found a maximum deficit of Br^- in summer. This was attributed to the condensation of acid sulfur species onto the sea-salt aerosol, which has a summer peak which is well correlated with DMS emission flux. However, in their study the Cl^- loss was low.

Little consistent seasonal cycle is evident in secondary sulphur species for the predominantly terrestrial air masses. Under baseline conditions the seasonal cycles of median values and maximum values appear to oppose one another.

Contributions of fresh sea salt were largest in winter and spring for both the primarily terrestrial and baseline categories, but median values were typically higher under baseline conditions (due to the oceanic source term for this aerosol type).

3.4. Differences between radon-only and trajectory-derived baseline

A comparison of the distributions of baseline source-type fingerprints for Cape Grim $PM_{2.5}$ aerosols, as determined by wind

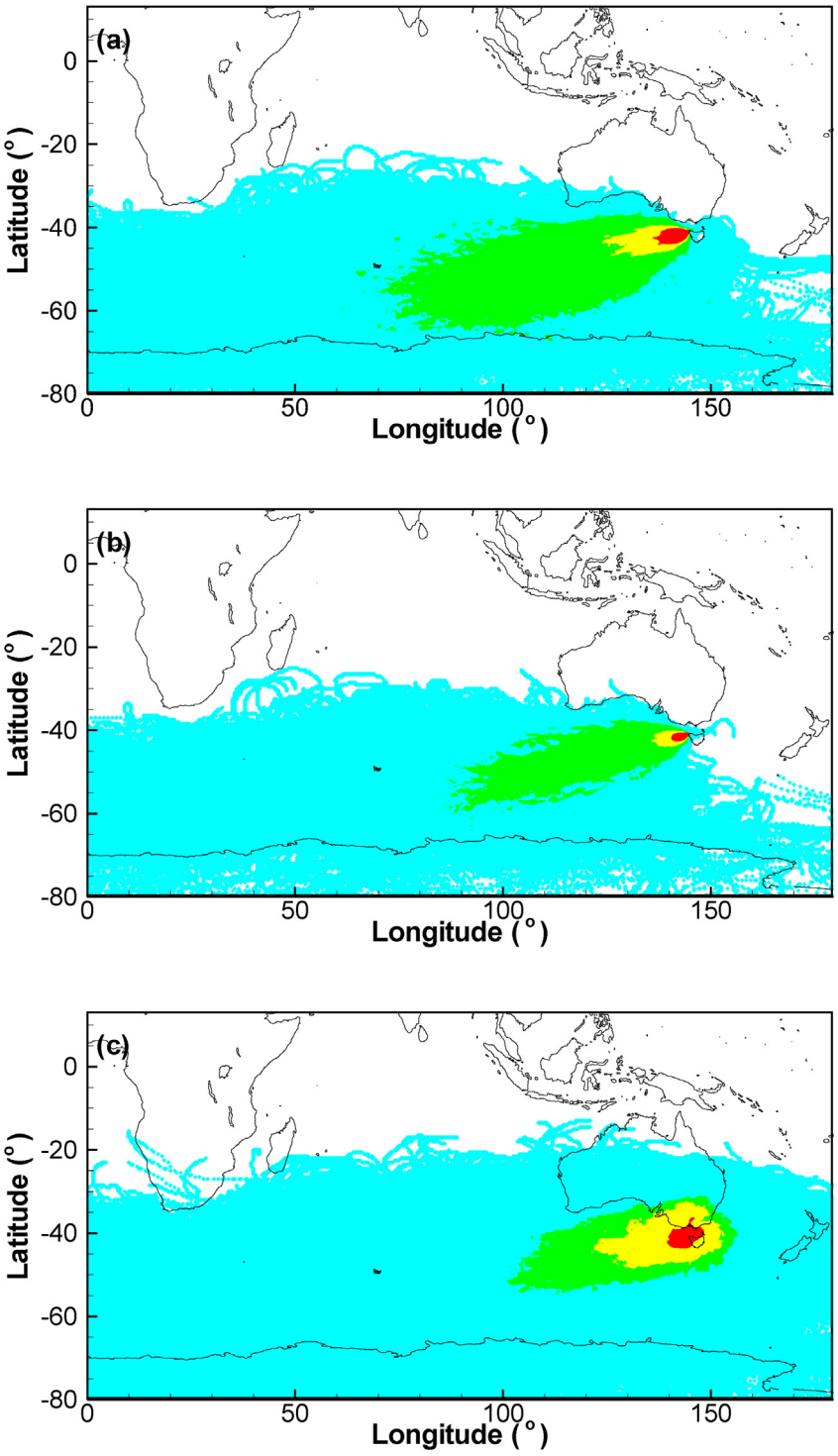

Fig. 5. Five day back trajectory density maps of hourly events corresponding to radon thresholds of (a) 100 mBq m^{-3}, (b) 50 mBq m^{-3}, and (c) for those days corresponding to Category 0 to 5 events.

direction/back trajectory analysis (Crawford et al., 2017) and by the radon-only baseline threshold (50 mBq m^{-3}) for category 6 (>20 h d^{-1} baseline) and category 7 (all baseline), are presented in Fig. 8.

Both radon-only baseline categories show higher concentrations of fresh sea salt, and lower concentrations of aged sea air and soil than the trajectory-based selection approach (Fig. 8). This gives credence to the (relaxed; i.e. category 6) radon-only baseline selection method, and demonstrates that baseline selection based predominantly on back trajectory analysis is not as selective at removing small amounts of terrestrial influence (presumably due to limitations in accuracy of the back trajectory calculations). However, this is not the whole story as the radon-only categories do not exhibit the narrower distributions that would be expected if they were excluding all the residual terrestrial effects. Interestingly, the soil, smoke, and industrial metals source fingerprints also

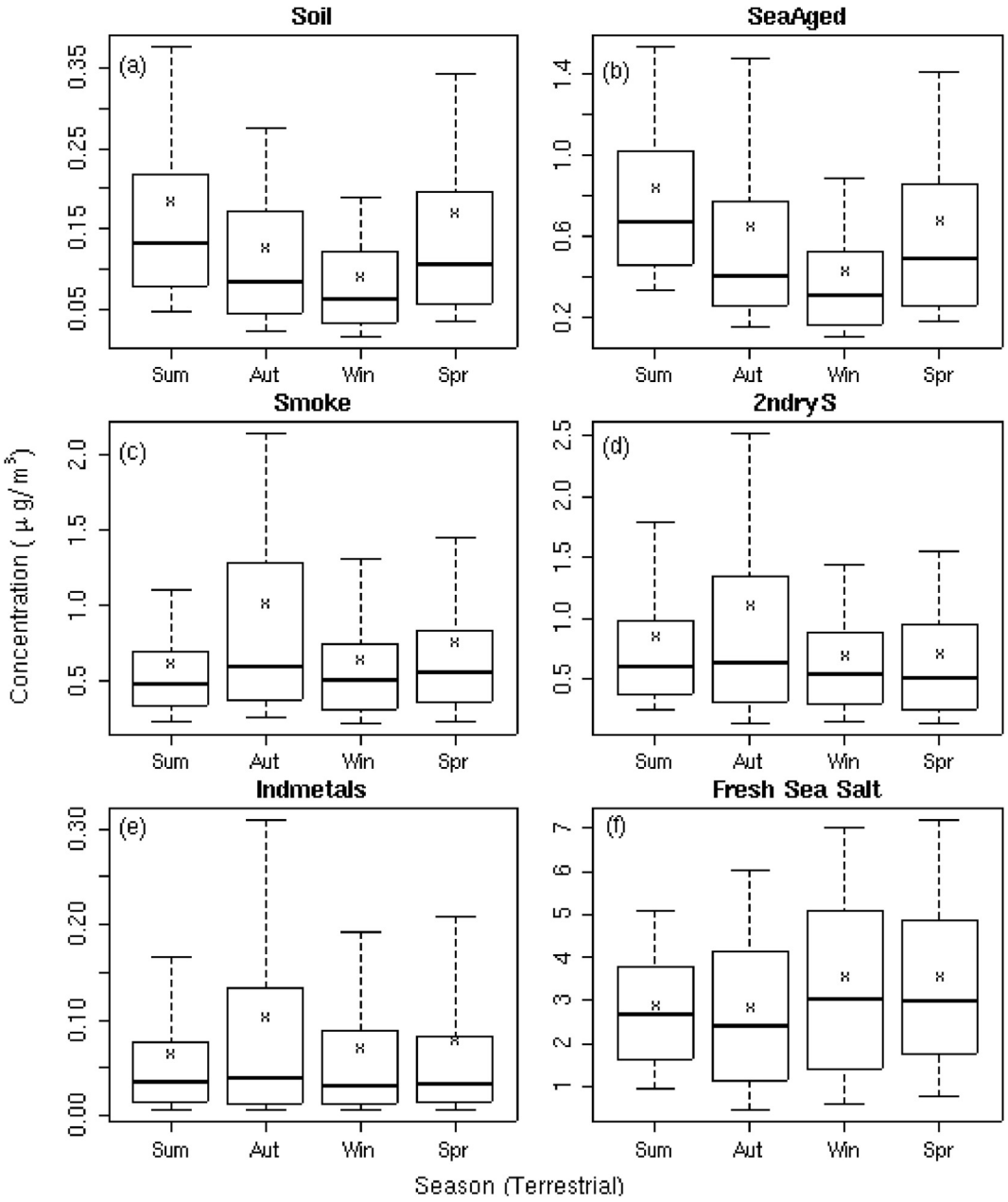

Fig. 6. Seasonal distributions of $PM_{2.5}$ source concentrations for category 0–5 events (≤20 h in baseline; or more terrestrially affected air masses) with the 50 mBq m^{-3} baseline radon threshold (symbols as in Fig. 1). (a) Soil, (b) SeaAged, (c) Smoke, (d) *2ndryS*, (e) Indmetals, and (f) Freash Sea Salt.

exhibit notably higher "extreme" (outlier) events associated with the radon-selected baseline samples than for the trajectory-selected samples (even for the category 7 events). Since radon is an unambiguous indicator of terrestrial influence, the most likely explanation for these observations is that a significant contribution to the smoke and industrial metal source fingerprints within Cape Grim baseline air masses derive from long-range transport (i.e. >3 weeks since last land contact).

A 10-day back-trajectory analysis of extreme smoke and industrial metal events (not shown) indicated that the outlier event air masses typically travelled at a lower altitude over the Southern Ocean than air masses for lesser magnitude events in the baseline category. However, due to increasing errors associated with the accuracy of back trajectories with duration (distance), these events were not traceable back ≥3 weeks in time to investigate potential origins of these signals.

4. Conclusions

An existing radon-only "baseline" air mass selection technique, based on hourly observations, was modified for use with daily-integrated $PM_{2.5}$ aerosol observations made by ANSTO at the Cape Grim Air Pollution Station between 2000 and 2015. To improve the compatibility of these results with previous studies two separate radon baseline selection threshold concentration values were used: 100 mBq m^{-3}, which has been used for decades (e.g., Gras and Whittlestone, 1992); and 50 mBq m^{-3} (Chambers et al., 2016; this study). Median aerosol concentrations were similar for both radon threshold values, but maximum concentrations were higher for air masses selected with the 100 mBq m^{-3}

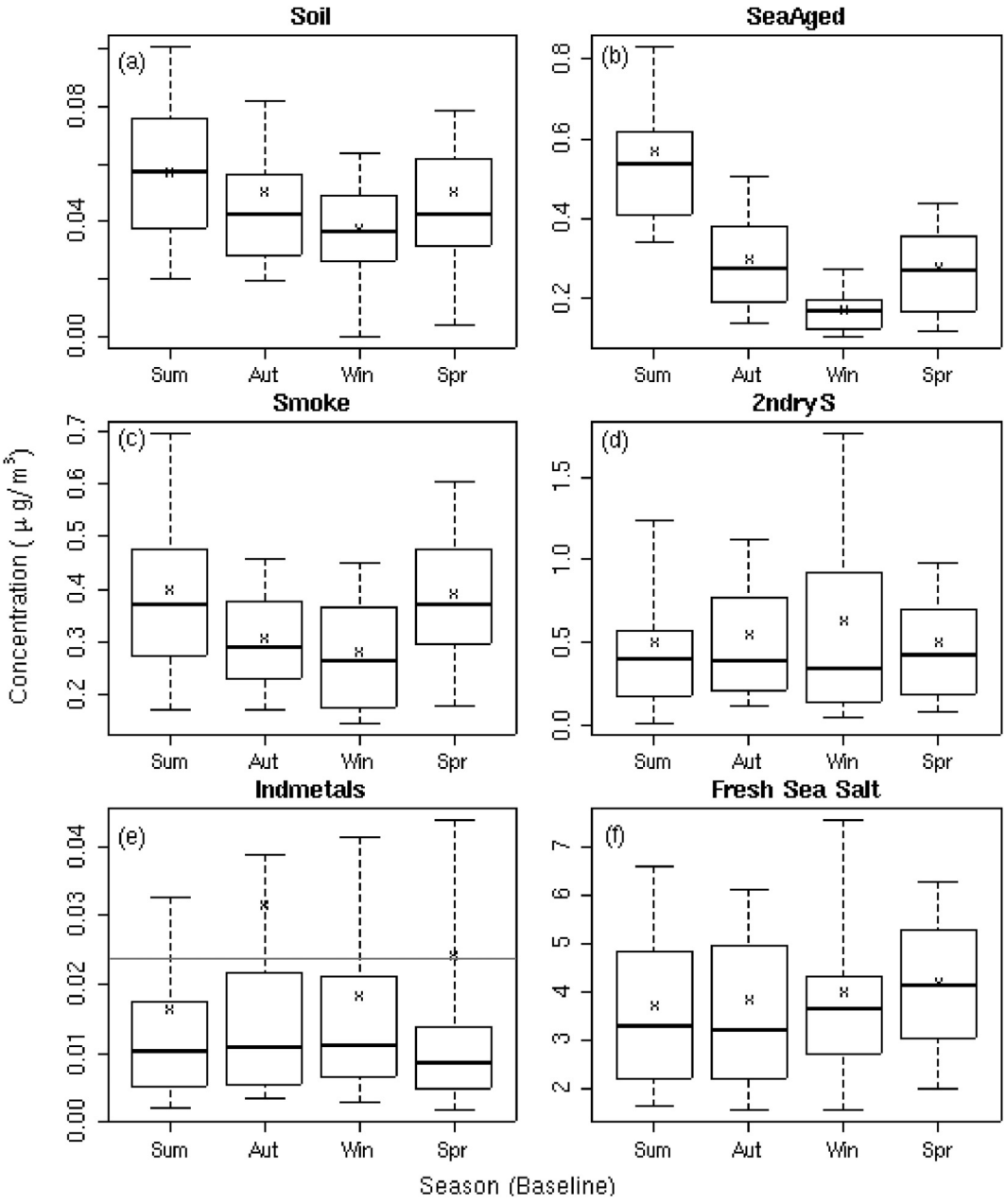

Fig. 7. Seasonal distributions of $PM_{2.5}$ source concentrations for category 6 events (>20 h in baseline; i.e. baseline samples) with the 50 mBq m^{-3} baseline radon threshold (symbols as in Fig. 1). (a) Soil, (b) SeaAged, (c) Smoke, (d) *2ndryS*, (e) Indmetals, and (f) Freash Sea Salt.

threshold. Back trajectory analyses demonstrated more frequent fleeting contact with southern Australia and Antarctic coastal regions (where there is exposed rock) for air masses selected with the 100 mBq m^{-3} threshold. The daily-integrated aerosol concentration statistics were not found to be significantly different when the baseline requirement was relaxed from all 24 h per day to >20 h d^{-1} beneath the radon baseline threshold concentration. This slight relaxation in baseline selection requirements increased the number of viable baseline aerosol sample days by almost a factor of two.

IBA and PMF techniques identified six contributing source-type fingerprints for the Cape Grim $PM_{2.5}$ aerosol: fresh sea salt (57%), secondary sulfate (14%), smoke (13%), aged sea salt (12%), soil dust (2.4%) and industrial metals (1.5%). Based on the 50 mBq m^{-3} radon baseline threshold concentration, the ratio of concentrations between terrestrial and baseline fetch conditions was 0.6, 1.9, 2.2, 2.6, 3.4, 5.5 for fresh sea salt, secondary sulphur, aged sea air, smoke, soil and industrial metals, respectively.

Radon-only baseline selection of the source-type fingerprints using the 50 mBq m^{-3} threshold was found to be more selective of minimal terrestrial influence than a similar recent study using wind direction and back trajectories to select baseline events (Crawford et al., 2017). Seasonal cycles of soil dust for both terrestrial and baseline fetch had a summer maximum and winter minimum, with a median amplitude that reduced from 0.07 μg m^{-3} under terrestrial fetch to 0.02 μg m^{-3} under baseline conditions. Seasonal cycles of smoke were of similar median amplitude for terrestrial and baseline events, but of completely different shape: peaking in autumn and spring for terrestrial events, compared to summer for baseline conditions. Seasonal cycles of industrial metals had a summer maximum and winter minimum, with a baseline

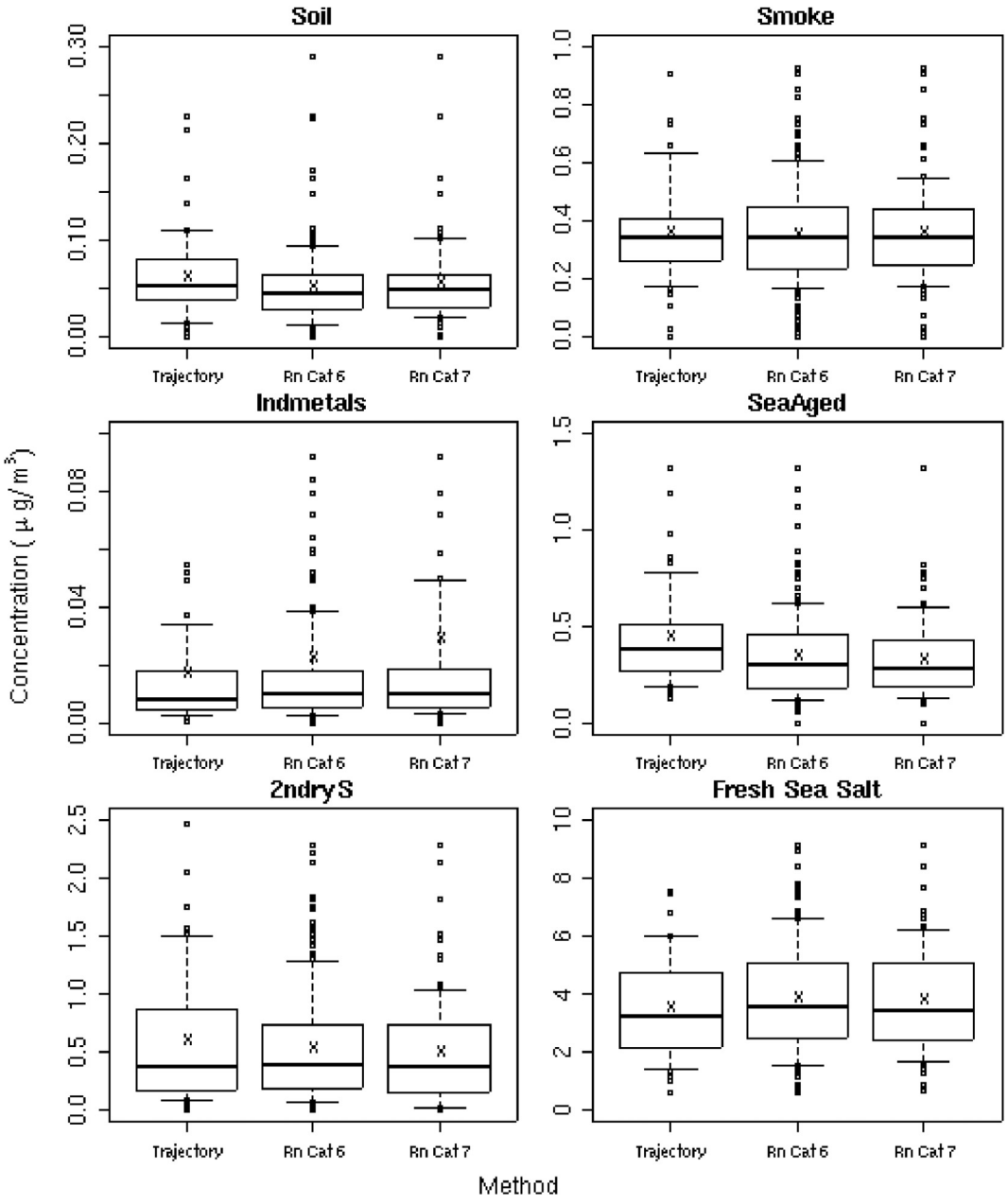

Fig. 8. Distributions (box and whisker plots as for Fig. 2) source-type fingerprints for the Cape Grim $PM_{2.5}$ aerosol under baseline conditions compared between the trajectory method of Crawford et al. (2017), and category 6 and 7 events of this study.

amplitude around a factor of 4 less than for terrestrial air masses. A significant fraction of the Cape Grim baseline smoke and industrial metal contributions appeared to derive from long-term transport (>3 weeks since last terrestrial influence).

Acknowledgments

The authors would like to acknowledge NCRIS funding for accelerators and Centre for Accelerator Science staff for access to their ion beam analysis facilities. The NOAA Air Resources Laboratory (ARL) made available the HYSPLIT transport and dispersion model. Also, thanks to the Cape Grim staff for their role in collecting the samples at the station over these many years, the radon group at ANSTO, and Dr Fabienne Reisen and Dr Melita Keywood from Commonwealth Scientific and Industrial Research Organization (CSIRO) for valuable comments on an earlier draft of the manuscript.

Appendix A. Supplementary data

Supplementary data related to this article can be found at https://doi.org/10.1016/j.envpol.2018.08.043.

References

Ayers, G.P., Ivey, J.P., 1988. Precipitation composition at Cape Grim, 1977-1985. Tellus 40B, 297–307.
Ayers, G.P., Cainey, J.M., Gillett, R.W., Saltzman, E.S., Hooper, M., 1997. Sulfur dioxide and dimethyl sulphide in marine air at Cape Grim, Tasmania. Tellus 49B, 292–299.
Ayers, G.P., Gillett, R.W., Cainey, J.M., Dick, A.L., 1999. Chloride and Bromide loss from sea-Salt particles in Southern Ocean air. J. Atmos. Chem. 33, 299–319.

Chambers, S.D., Williams, A.G., Crawford, J., Griffiths, A.D., Krummel, P.B., Steele, L.P., Law, R.M., van der Schoot, M.V., Galbally, I.E., Molloy, S.B., 2018. A radon-only technique for characterising "baseline" constituent concentrations at Cape Grim. In: Derek, N., Krummel, P.B., Cleland, S.J. (Eds.), Baseline Atmospheric Program Australia 2011-2013. Australian Bureau of Meteorology and CSIRO Marine and Atmospheric Research (in press). https://www.researchgate.net/publication/280028388_A_RADON-ONLY_TECHNIQUE_FOR_CHARACTERISING_ATMOSPHERIC_%27BASELINE%27_CONSTITUENT_CONCENTRATIONS_AT_CAPE_GRIM.

Chambers, S.D., Williams, A.G., Conen, F., Griffiths, A.D., Reimann, S., Steinbacher, M., Krummel, P.B., Paul Steele, L., van der Schour, M.V., Galbally, I.E., Molloy, S.B., Barnes, J.E., 2016. Towards a universal "baseline" characterisation of air masses for high- and low-altitude observing stations using Radon-222. Aerosol Air Qua. Res 16, 885–890.

Chambers, S.D., Zahorowski, W., Williams, A.G., Crawford, J., Griffiths, A.D., 2013. Identifying tropospheric baseline air masses at Mauna Loa Observatory between 2004 and 2010 using Radon-222 and back trajectories. J. Geophys. Res. Atmos. 118 https://doi.org/10.1029/2012JD018212.

Chambers, S.D., Hong, S.B., Williams, A.G., Crawford, J., Griffiths, A.D., Park, S.J., 2014. Characterising terrestrial influences on Antarctic air masses using Radon-222 measurements at King George Island. Atmos. Chem. Phys. 14, 9903–9916.

Cleland, S.J., 2014. Meteorology/climatology 2009-2010. In: Derek, N., Krummel, P.B., Cleland, S.J. (Eds.), Baseline Atmospheric Program Australia 2009-2010. Australian Bureau of Meteorology and CSIRO Marine and Atmospheric Research, pp. 27–32.

Cohen, D.D., Bailey, G.M., Kondepudi, R., 1996. Elemental analysis by PIXE and other IBA techniques and their application to source fingerprinting of atmospheric fine particle pollution. Nucl. Instrum. Methods 109, 218–226.

Crawford, J., Cohen, D.D., Stelcer, E., Atanacio, A., 2017. Long term fine aerosols at the Cape Grim global baseline station: 1998 to 2016. Atmos. Environ. 166, 34–46.

Draxler, R., Stunder, B., Rolph, G., Stein, A., Taylor, A., 2016. HYSPLIT4 USER's GUIDE Version 4 - Last Revision: February 2016. https://www.arl.noaa.gov/documents/reports/hysplit_user_guide.pdf.

Faloona, I., 2009. Sulfur processing in the marine atmospheric boundary layer: a review and critical assessment of modelling uncertainties. Atmos. Environ. 43, 2841–2854.

Fleming, Z.L., Monkis, P.S., Manning, A.J., 2012. Review: untangling the influence of air-mass history in interpreting observed atmospheric composition. Atmos. Res. 104–105, 1–39.

Galbally, I.E., Schultz, M.G., 2013. Guidelines for Continuous Measurement of Ozone in the Troposphere, *GAW Report No. 209*. Publication WMO-No. 1110, ISBN 978-92-63-11110-4. World Meteorological Organisation, Geneva, Switzerland, p. 76.

Giemsa, E., Jacobeit, J., Rie, L., Hachinger, S., Meyer-Arnek, J., 2017. Application of Trajectory Clustering and Source Attribution Methods for Investigating Regional CO2 Concentrations at Germany's Highest Mountain Site. Jahrestagung des Arbeitskreis Klima. Schloss Rauischholzhausen, Germany, pp. 27–29.

Gras, J.L.S., Whittlestone, S., 1992. Radon and CN: complementary tracers of polluted air masses at coastal and island sites. J. Radioanal. Nucl. Chem. 161 (1), 293–306.

Griffiths, A., Chambers, S.D., Williams, A.G., Werczynski, S., 2016. Increasing the accuracy and temporal resolution of two-filter radon-222 measurements by correcting for the instrument response. Atmos Meas Tech 9, 2689–2707.

Hyslop, N.P., Trzepla, K., Wallis, C.D., Matzoll, A.K., White, W.H., 2013. Technical note: a 23-year record of twice-weekly aerosol composition measurements at Mauna Loa Observatory. Atmos. Environ. 80, 259–263.

Li, F., Ginoux, P., Ramaswamy, V., 2008. Distribution, transport, and deposition of mineral dust in the Southern Ocean and Antarctica: contribution of major sources. J. Geophys. Res. 113, D10207.

Liang, C.-S., Duan, F.-K., He, K.-B., Ma, Y.-L., 2016. Review on recent progress in observations, source identifications and countermeasures of $PM_{2.5}$. Environ. Int. 86, 150–170.

Liu, S.C., McAfee, J.R., Cicerone, R.J., 1984. Radon-222 and tropospheric vertical transport. J. Geophys. Res. 89, 7291–7297.

Mari, C.H., Cailley, G., Corre, L., Saunois, M., Attié, J.L., Thouret, V., Stohl, A., 2008. Tracing biomass burning plumes from the Southern Hemisphere during the AMMA 2006 wet season experiment. Atmos. Chem. Phys. 8, 3951–3961.

Molloy, S.B., Galbally, I.E., 2014. Analysis and identification of a suitable baseline definition of tropospheric ozone at Cape Grim, Tasmania. In: Derek, N., Krummel, P.B., Cleland, S.J. (Eds.), Baseline Atmospheric Program Australia 2009-2010. Australian Bureau of Meteorology and CSIRO Marine and Atmospheric Research, pp. 7–16. June 2014.

Paatero, P., Tapper, U., 1994. Positive Matrix Factorisation: a non-negative factor model with optimal utilisation of error estimates of data values. Environmetrics 5, 111–126.

Polian, G., Lambert, G., Ardouin, B., Jegou, A., 1986. Long-range transport of continetal radon in subantarctic and actic areas. Tellus 38, 178–189.

Rotstayn, L.D., Keywood, M.D., Forgan, B.W., Gabric, A.J., Galbally, I.E., Gras, J.L., Luhar, A.K., McTainsh, G.H., Mitchell, R.M., Young, S.A., 2009. Possible impacts of anthropogenic and natural aerosols on Australian climate: a review. Int. J. Climatol. 29, 461–479.

Schery, S.D., Whittlestone, S., Hart, K.P., Hill, S.E., 1989. The flux of radon and thoron from australian soils. J. Geophys. Res. 94, 8567–8576.

Station Specification, 2014. General. In: Derek, N., Krummel, P.B., Cleland, S.J. (Eds.), Baseline Atmospheric Program Australia 2009-2010. Australian Bureau of Meteorology and CSIRO Marine and Atmos Res, pp. 1–2. June 2014.

Stein, A.F., Draxler, R.R., Rolph, G.D., Stunder, B.J.B., Cohen, M.D., Ngan, F., Dec 2015. Free access NOAA's HYSPLIT atmospheric transport and dispersion modeling system. Bull. Am. Meteorol. Soc. 2059–2077. https://doi.org/10.1175/BAMS-D-14-00110.1.

Sustainable Timber Tasmania 2017. https://www.sttas.com.au/forest-operations-management/our-operations/planned-burns.

Thoning, K.W., Tans, P.P., Komhyr, W.D., 1989. Atmospheric carbon-dioxide at Mauna Loa observatory, 2. Analysis of the NOAA GMCC data, 1974-1985. J. Geophys. Res. Atmos. 94, 8549–8565.

Weller, R., Minikin, A., Petzold, A., Wagenbach, D., Kőnig-Langlo, G., 2013. Characterization of long-term and seasonal variations of black carbon (BC) concentrations at Neumayer, Antarctica. Atmos. Chem. Phys. 13, 1579–1590.

Whittlestone, S., Zahorowski, W., 1998. Baseline radon detectors for shipboard use: development and deployment in the first Aerosol Characterization Experiment (ACE 1). J Geophys Res Atm 103, 16743–16751.

Wilkening, M.H., Clements, W.E., 1975. Radon 222 from the ocean surface. J. Geophys. Res. 80, 3828–3830.

Williams, A.G., Chambers, S.D., 2016. A History of Radon Measurements at Cape Grim, *Baseline Atmospheric Program (Australia) History and Recollections*, pp. 131–146 (40th Anniversary Special Edition).

Williams, A.G., Chambers, S.D., Griffiths, A.D., Loh, Z.M., Krummel, P.B., 2017. Seasonal variations in 'deep baseline' radon over the Southern Ocean. In: Murramarang, N.S.W., Derek, N., Krummel, P.B. (Eds.), Atmospheric Composition & Chemistry Observations & Modelling Conference Incorporating the Cape Grim Annual Science Meeting 2017 [oral], 8-10 November 2017. Bureau of Meteorology and CSIRO Oceans and Atmosphere, Climate Science Centre, Melbourne, Australia, p. 10.

WMO, 1978. International Operations Handbook for Measurement of Background Atmospheric Pollution. World Meteorological Organisation, Geneva. No, 491, 110.

WMO/GAW, 2017. WMO Global Atmosphere Watch (GAW) Implementation Plan: 2016 – 2023. GAW Report No. 228.

Zahorowski, W., Griffiths, A.D., Chambers, S.D., Williams, A.G., Law, R.M., Crawford, J., Werczynski, S., 2013. Constraining annual and seasonal Radon-222 flux density from the Southern Ocean using Radon-222 concentrations in the boundary layer at Cape Grim. Tellus B 65, 19622. https://doi.org/10.3402/tellusb.v65i0.19622.